Search for sphalerons in proton-proton collisions

John Ellis[a,b] **and Kazuki Sakurai**[c]

[a] *Theoretical Particle Physics and Cosmology Group,*
Physics Department, King's College London,
London WC2R 2LS, U.K.

[b] *Theoretical Physics Department, CERN,*
CH-1211 Geneva 23, Switzerland

[c] *Institute for Particle Physics Phenomenology,*
Department of Physics, University of Durham, Science Laboratories,
South Road, Durham, DH1 3LE, U.K.

E-mail: John.Ellis@cern.ch, kazuki.sakurai@durham.ac.uk

ABSTRACT: In a recent paper, Tye and Wong (TW) have argued that sphaleron-induced transitions in high-energy proton-proton collisions should be enhanced compared to previous calculations, based on a construction of a Bloch wave function in the periodic sphaleron potential and the corresponding pass band structure. Here we convolute the calculations of TW with parton distribution functions and simulations of final states to explore the signatures of sphaleron transitions at the LHC and possible future colliders. We calculate the increase of sphaleron transition rates in proton-proton collisions at centre-of-mass energies of 13/14/33/100 TeV for different sphaleron barrier heights, while recognising that the rates have large overall uncertainties. We use a simulation to show that LHC searches for microscopic black holes should have good efficiency for detecting sphaleron-induced final states, and discuss their experimental signatures and observability in Run 2 of the LHC and beyond. We recast the early ATLAS Run-2 search for microscopic black holes to constrain the rate of sphaleron transitions at 13 TeV, deriving a significant limit on the sphaleron transition rate for the nominal sphaleron barrier height of 9 TeV.

Contents

1 Introduction

Non-perturbative effects in the electroweak sector of the Standard Model are predicted to violate baryon (B) and lepton (L) conservation, violating the combination $B + L$ while conserving $B - L$. The first example was provided by electroweak instantons [1], which yield $\Delta B = 3$ transitions that are suppressed to unobservable levels by factors $\sim \exp(-2\pi/\alpha_W)$, where $\alpha_W = g_W^2/4\pi$ is the SU(2) coupling strength. The second example was provided by sphalerons [2, 3], which are classical solutions of the electroweak field equations that interpolate between vacua with different values of the Chern-Simons number, providing a potential barrier E_{Sph} to $\Delta B = 3$ transitions that is expected to be $\simeq 9\,\mathrm{TeV}$. It has been thought that experimental observation of sphaleron-induced transitions would also be unobservable at the LHC [4–11], because $\Delta n = \pm 1$ transitions would be suppressed by $\exp(\mathcal{O}(-4\pi/\alpha_W))$.[1]

    However, this longstanding consensus has been challenged in a bold recent paper [14] by S.-H. Henry Tye and Sam S. C. Wong (TW), who argue that sphaleron-induced transition rates could be much larger than had been estimated previously. They argue that an essential element in calculating the rate of $\Delta n \neq 0$ transitions is the periodic nature of the effective Chern-Simons potential, which should be taken into account by constructing the corresponding Bloch wave function. Their approach leads to a band structure for transitions through the sphaleron barrier, resulting in a reduced suppression at energies $< E_{\mathrm{Sph}}$ that disappears entirely at energies $\geq E_{\mathrm{Sph}}$. As stressed in [14], this remarkable claim raises the possibility that sphaleron-induced transitions might be observable at the LHC and higher-energy proton-proton colliders. The experimental observation of such

---

[1]Some other calculations [12, 13] have, however, also suggested that this exponential suppression disappears at partonic centre-of-mass energies around $30\,\mathrm{TeV}$, and that instanton-induced processes may be observable at very high energy pp colliders with $\sqrt{s} \gtrsim 100\,\mathrm{TeV}$.

transitions would not only be a beautiful confirmation of profound theoretical insights, but would also have important cosmological implications, since sphalerons are thought to have played an essential rôle in generating the baryon asymmetry of the Universe [11, 15–20].

In this paper we follow up the suggestion of TW by calculating the energy dependence of the rates for sphaleron-induced transitions in proton-proton collisions, including the factors arising from quark parton distribution functions, and use simulations of their possible final states to study the possible signatures of such transitions. As stressed by TW, there are inevitable uncertainties in calculations of the rates for sphaleron-induced transitions, notably including the sphaleron barrier height E_{Sph}, the coefficient inside the exponential suppression, and any possible prefactor. That said, our calculations encourage us to explore how the rate for sphaleron-induced transitions might be constrained by experiments at the LHC, possibly during its Run 2 that has now started. Accordingly, we simulate the final states of sphaleron-induced transitions, demonstrating that the searches for microscopic black holes that have already been designed would have good acceptance for sphaleron-induced final states,[2] which would also possess additional distinctive signatures. As an illustration, we constrain sphaleron transition rates by recasting the results of the ATLAS Run-2 search for microscopic black holes using $\sim 3\,\mathrm{fb}^{-1}$ of data recorded at $13\,\mathrm{TeV}$ in 2015 [22]. We find that these data already exclude a pre-exponential transition rate factor of unity for the nominal sphaleron barrier height of $9\,\mathrm{TeV}$.

2 Theoretical background

It is argued in [14] that sphaleron transitions can be modelled by a one-dimensional Schrödinger equation of the form

$$\left(-\frac{1}{2m}\frac{\partial^2}{\partial Q^2} + V(Q)\right)\Psi(Q) = E\Psi(Q)\,, \tag{2.1}$$

where m is an effective "mass" parameter for the Chern-Simons number n whose value was first calculated in [14], $Q \equiv \mu/m_W$ where μ is defined implicitly by $n\pi = \mu - \sin(2\mu)/2$, and the effective potential is taken from [2]:

$$V(Q) \simeq 4.75 \left(1.31\sin^2(Qm_W) + 0.60\sin^4(Qm_W)\right)\,\mathrm{TeV}\,. \tag{2.2}$$

Two evaluations of m were discussed in [14]: one based on [2] that yielded the estimate $m = 17.1\,\mathrm{TeV}$, and the other based on [23] that yielded the estimate $m = 22.5\,\mathrm{TeV}$. The final results for the rate of sphaleron-induced transitions were very similar, and here we follow [14] in adopting the [2]-based calculation that led to $m = 17.1\,\mathrm{TeV}$.

The sphaleron barrier height E_{Sph} is given by

$$E_{\mathrm{Sph}} = \mathrm{Max}\,V(Q) = V\left(\frac{\pi}{2m_W}\right)\,. \tag{2.3}$$

---

[2]The similarity between the final states of sphaleron-induced transitions and mini black holes has been pointed out in [21].

In a pure SU(2) theory, one finds $E_{\text{Sph}} = 9.11 \, \text{TeV}$, and it is estimated that incorporating the U(1) of the Standard Model reduces this by $\sim 1\%$. Here we follow [14] in assuming a nominal value of $E_{\text{Sph}} = 9 \, \text{TeV}$, while presenting some numerical results for the alternative choices $E_{\text{Sph}} = 8, 10 \, \text{TeV}$. Later, we also use a recast of early Run-2 searches for microscopic black holes to constrain the sphaleron transition rate as a function of E_{Sph}.

As was discussed in detail in [14], the Bloch wave function for the periodic potential (2.2) is straightforwardly obtained, and the corresponding conducting (pass) bands can be calculated, as well as their widths and the gaps between the bands. The lowest-lying bands are very narrow, but the widths increase with the heights of the bands. Averaging over the energies $E_{1,2}$ of the colliding quark partons yields a strong suppression at $E_1 + E_2 \ll E_{\text{Sph}}$, which corresponds to the exponential suppression found in a conventional tunnelling calculation. However, this suppression decreases as $E_1 + E_2 \to E_{\text{Sph}}$, and there is no suppression for $E_1 + E_2 \geq E_{\text{Sph}}$.

The result of the analysis in [14] can be summarized in the partonic cross-section

$$\sigma(\Delta n = \pm 1) \;\propto\; \exp\left(c \frac{4\pi}{\alpha_W} S(E) \right) , \tag{2.4}$$

where E is the centre-of-mass energy of the parton-parton collision, $c \sim 2$ and the suppression factor $S(E)$ is shown in figure 8 of [14]. As seen there, it rises from the value $S(E) = -1$ in the low-energy limit ($E \ll E_{\text{Sph}}$) to $S(E) = 0$ for energies $E \geq E_{\text{Sph}}$, with very similar results being found in [14] for calculations based on the work of [2] and [23]. For the purpose of our numerical calculations, we approximate $S(E)$ at intermediate energies by

$$S(E) = (1 - a)\hat{E} + a\hat{E}^2 - 1 \quad \text{for} \quad 0 \leq \hat{E} \leq 1 , \tag{2.5}$$

where $\hat{E} \equiv E/E_{\text{Sph}}$ and $a = -0.005$.

The overall magnitude of eq. (2.4) is not given. We speculate that the relevant scale should be proportional to the non-perturbative electro-weak cross-section for q-q scattering, σ_{qq}^{EW}. Analogously to the fact that the inelastic p-p cross-section is given roughly by $\sim 1/m_\pi^2$, we take $\sigma_{qq}^{\text{EW}} \sim 1/m_W^2$. Our cross-section formula is, thus, given as

$$\sigma(\Delta n = \pm 1) = \frac{1}{m_W^2} \sum_{ab} \int dE \frac{d\mathcal{L}_{ab}}{dE} \; p \; \exp\left(c \frac{4\pi}{\alpha_W} S(E) \right) , \tag{2.6}$$

where p is an unknown factor (that might well depend[3] on the subprocess energy E) and $\frac{d\mathcal{L}_{ab}}{dE}$ is the parton luminosity function of the colliding quarks a and b, which are obtained from the parton distribution functions at a momentum fraction x, $f_a(x)$, evaluated at the appropriate energy scale E:

$$\frac{d\mathcal{L}_{ab}}{dE} = \frac{2E}{E_{\text{CM}}^2} \int_{\ln \sqrt{\tau}}^{-\ln \sqrt{\tau}} dy f_a(\sqrt{\tau} e^y) f_b(\sqrt{\tau} e^{-y}), \tag{2.7}$$

where E_{CM} is the centre-of-mass energy of the p-p collision and $\tau = E^2/E_{\text{CM}}^2$.

---

[3]S.-H. Henry Tye and Sam S.C. Wong, private communication and to appear.

3 Cross-section calculations

We include in our calculations collisions of all quarks in the lightest two generations, namely u, d, s and c. We recall that only left-handed (SU(2) doublet) quarks are active in inducing sphaleron transitions, so that the usual unpolarized quark-quark parton collision luminosity functions must be reduced by a factor 4. Additionally, we expect that quarks in the same generation must collide in an antitriplet state, reducing the corresponding luminosity functions by another factor 3. In principle, one should also incorporate Cabibbo mixing, but this is unimportant compared with the uncertainties in the calculation.

The upper panel of figure 1 displays the relative contributions of the collisions of different quark flavours for the nominal case $E_{\mathrm{CM}} = 14\,\mathrm{TeV}$, $E_{\mathrm{Sph}} = 9\,\mathrm{TeV}$, $c = 2$, with the normalization corresponding to $p = 1$ in (2.6). We see that, as expected, the dominant contribution to the sphaleron cross section is due to uu collisions, with ud collisions being the second most important, and other processes contributing $< 3\%$ of the total. Sphaleron production by collisions involving d quarks are suppressed at $14\,\mathrm{TeV}$ because the u parton distribution function is much larger than that for the d quark at large momentum fraction x.

The lower panels of figure 1 display the corresponding relative contributions of different quark flavours for $E_{\mathrm{CM}} = 13, 33$ and $100\,\mathrm{TeV}$. As could be expected, the relative contributions at $13\,\mathrm{TeV}$ are quite similar to those at $14\,\mathrm{TeV}$, but the dominance of uu and ud collisions is challenged increasingly at 33 and $100\,\mathrm{TeV}$ by transitions induced by dd collisions and processes involving second-generation quarks.

Our calculations of the E_{CM} dependence of the sphaleron cross section are displayed in figure 2. The solid curve is for the nominal choices $E_{\mathrm{Sph}} = 9\,\mathrm{TeV}$, $c = 2$ and constant $p = 1$.[4] Results for values of the parameter $c \in [1, 4]$ in (2.6) are indistinguishable, as could have been anticipated from the steep fall-off of the sphaleron cross section for $E < E_{\mathrm{Sph}}$ seen in figure 1. We see that the cross section is substantial already at LHC energies *if* $p = 1$: specifically we calculate $\sigma = 7.3\,\mathrm{fb}$ for $E_{\mathrm{CM}} = 13\,\mathrm{TeV}$ and $\sigma = 41\,\mathrm{fb}$ for $E_{\mathrm{CM}} = 14\,\mathrm{TeV}$. However, the value of p must be regarded as *very uncertain*, and these numbers would be reduced substantially if the unknown parameter $p \ll 1$, a possibility that could only be countered (partially) by increasing E_{CM}. The steep rise in the cross section by a factor ~ 6 between $E_{\mathrm{CM}} = 13$ and $14\,\mathrm{TeV}$ is largely independent of c and p, and puts a premium on developing and exploiting the full energy capability of the LHC. However, the size of the cross section for sphaleron-induced processes for the nominal choice $p = 1$ suggests that it would be interesting to look for them during LHC Run 2, even with just a few fb^{-1} of luminosity at $13\,\mathrm{TeV}$ as already accumulated.

The dot-dashed and dashed curves in figure 2 are for the cases $E_{\mathrm{Sph}} = 8$ and $10\,\mathrm{TeV}$, which lie far outside the uncertainty in $E_{\mathrm{Sph}} \sim 1\%$ quoted in [14]. It is clear that the LHC cross section is smaller for larger E_{Sph}, and the energy dependence is steeper, whereas the opposite statements hold for smaller E_{Sph}. However, whereas in the former case sphaleron-induced processes could be more visible in Run 2 of the LHC, even in the latter case increasing E_{CM} should be a priority for the LHC.

---

[4]As already commented, p might depend on the subprocess energy E, which would modify the centre-of-mass energy dependence.
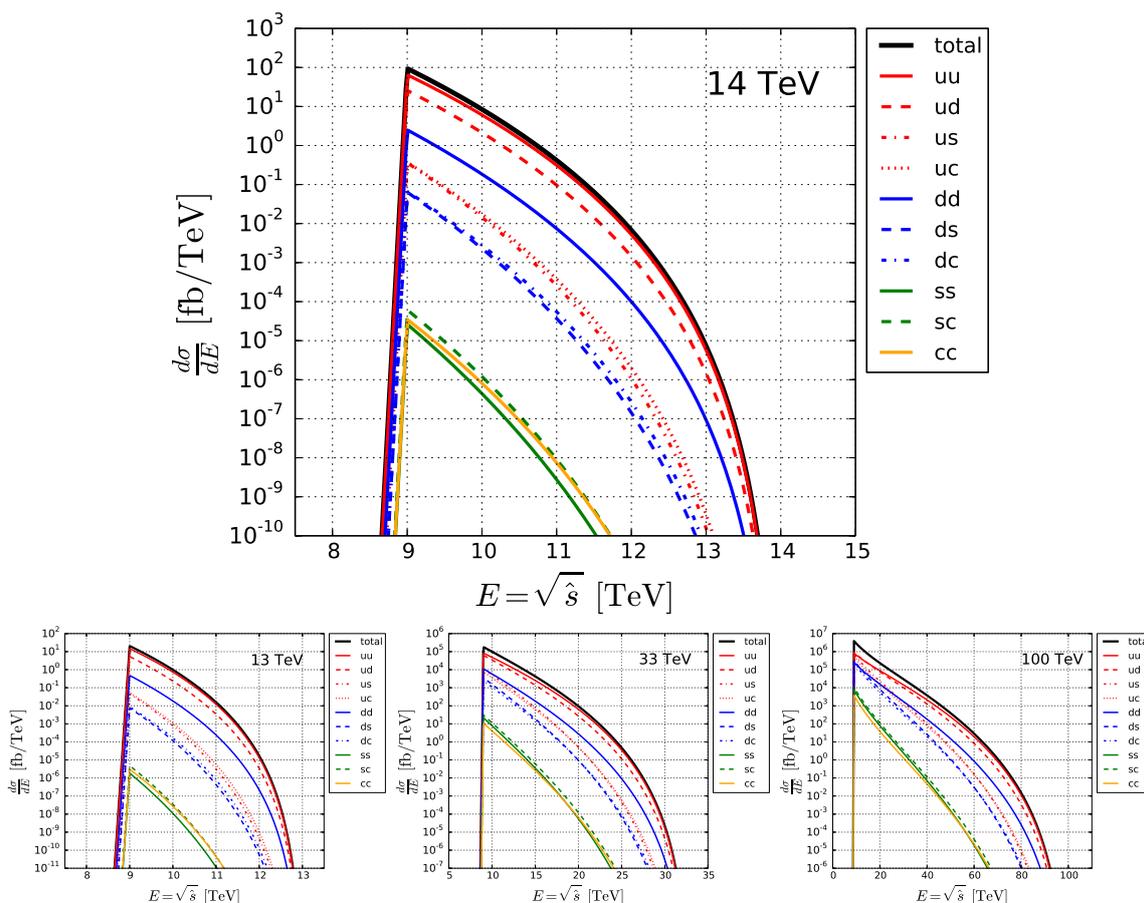
Figure 1. Upper panel: contributions to the cross section for sphaleron transitions from the collisions of different flavours of quarks, for the nominal case $E_{\rm CM} = 14\,{\rm TeV}$, $E_{\rm Sph} = 9\,{\rm TeV}$, $c = 2$ and $p = 1$ in (2.6) with S given by (2.5). The contributions of different parton-parton collision processes are colour-coded as indicated. Lower panels: as above, for the cases $E_{\rm CM} = 13, 33$ and $100\,{\rm TeV}$.

Looking beyond the LHC, figure 2 shows that the sphaleron transition rate would increase significantly at colliders with higher $E_{\rm CM}$. Specifically, for our nominal choices $E_{\rm Sph} = 9\,{\rm TeV}$, $c = 2$ and $p = 1$ we find sphaleron cross sections $0.3\,(141) \times 10^6$ fb at $E_{\rm CM} = 33\,(100)\,{\rm TeV}$. These can be compared with the expected $gg \to H$ cross sections at these centre-of-mass energies, which are $0.18\,(0.74) \times 10^6$ fb at 33 (100) TeV. If these estimates are in the right ball-park, such higher-energy colliders would be veritable sphaleron factories. However, we emphasize again that the overall magnitude of the sphaleron transition rate is *very uncertain*. One should, perhaps, instead regard figure 2 as showing that higher-energy collisions may provide sensitivity to sphaleron transitions for $p \ll 1$.

4 Simulations of sphaleron-induced processes

We turn now to the prospective observability of sphaleron-induced processes, the simplest possibility being $\Delta n = -1$ processes that give rise to effective interactions involving one
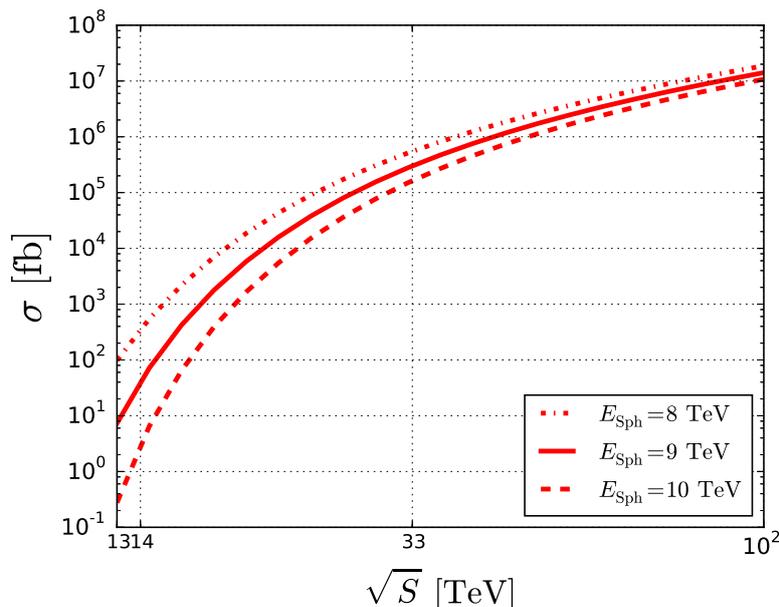
Figure 2. The energy dependence of the total cross section for sphaleron transitions for the nominal choices $E_{\rm Sph} = 9\,{\rm TeV}$, $c = 2$ and $p = 1$ in (2.6) with S given by (2.5) (solid curve), and for the outlying choices $E_{\rm Sph} = 8$ and $10\,{\rm TeV}$ (dot-dashed and dashed lines, respectively). The variations in the curves for $1 \leq c \leq 4$ are within the widths of the lines. We recall that the overall normalization factor p is quite uncertain.

member of each electroweak doublet, i.e., e/ν_e, μ/ν_μ, τ/ν_τ, and 3 colours of u/d, c/s and t/b, leading to transitions of the form

$$ qq \rightarrow \bar{\ell}\,\bar{\ell}\,\bar{\ell}\,\bar{q}\,\bar{q}\,\bar{q}\,\bar{q}\,\bar{q}\,\bar{q}\,\bar{q}. \tag{4.1} $$

A priori, the leading-order sphaleron-induced processes do not involve electroweak bosons.[5] Since the dominant processes are induced by uu and ud collisions: the final states should contain a single $\bar{u}/\bar{d}$ antiquark, one antilepton from each generation, three $\bar{c}/\bar{s}$ antiquarks and three $\bar{t}/\bar{b}$ antiquarks, for a total of 10 final state particles. The initial and final states are constrained so that the total electric charge is conserved. We make parton-level simulations, with the momenta of final-state particles given by phase space.[6] We also simulate the decays of heavy particles (t, W and τ). We accept only particles with $p_T > 20$ and $|\eta| < 2.5$. Neutrinos are removed from the list of observable particles.

The normalized invariant-mass distributions for the observable final-state particles are shown in figure 3, for LHC collisions at 13 and 14 TeV (left panel, blue and red histograms, respectively) and for future colliders at 33 and 100 TeV (right panel, green and pink histograms, respectively), for our nominal choices $E_{\rm Sph} = 9\,{\rm TeV}$, $c = 2$ and $p = 1$. As seen in

---

[5]There are suggestions that the baryon and lepton number violating processes are enhanced if fermions are produced associated with many $\mathcal{O}(1/\alpha_W)$ electroweak bosons [5, 6, 24–26]. We leave the investigation of this possibility for future work.

[6]We use our own code to simulate sphaleron-induced processes. There is also a public Monte Carlo tool to simulate sphaleron events [27].
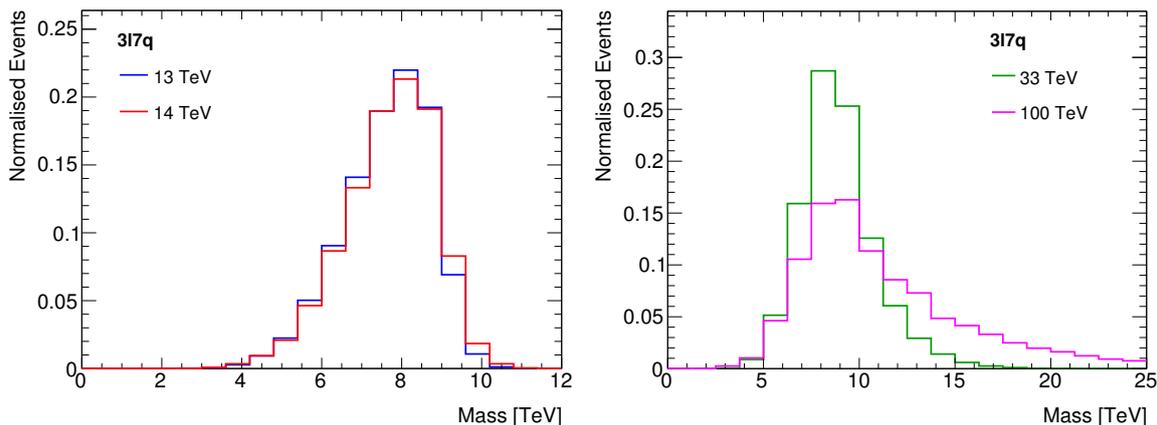
Figure 3. Left panel: normalized invariant-mass distributions for the observable final-state particles in sphaleron-induced transitions in LHC collisions at 13 and 14 TeV (blue and red histograms, respectively). Right panel: corresponding invariant-mass distributions for future colliders at 33 and 100 TeV (green and pink histograms, respectively). These distributions are calculated for our nominal choices $E_{\mathrm{Sph}} = 9\,\mathrm{TeV}$, $c = 2$ and $p = 1$.

the left panel, the invariant-mass distributions for 13 and 14 TeV are quite similar, both being peaked at $\sim 8\,\mathrm{TeV}$ and with tails extending to lower masses, corresponding to events with (multiple) neutrino emission. As seen in the right panel, the corresponding distributions for collisions at 33 and (particularly) 100 TeV extend to much larger invariant masses.

Figure 4 displays some more properties of the final states in sphaleron-induced transitions: the red histograms are for the $\Delta n = -1$ processes leading to 10-particle final states discussed above (4.1). One should also consider processes with other values of Δn, the next simplest being the $\Delta n = +1$ process that leads to 14-particle final states:

$$q\,q \; \to \; \ell\,\ell\,\ell\,q\,q\,q\,q\,q\,q\,q\,q\,q\,q\,q, \tag{4.2}$$

whose simulation yields the blue histograms in figure 4. The difference between these nominal multiplicities is visible in the upper left panel. The multiplicity may exceed the nominal value if gluon radiation or other higher-order QCD processes yield additional final-state partons satisfying our chose acceptance cuts: $p_T > 20\,\mathrm{GeV}$ and $|\eta| < 2.5$. On the other hand, the visible multiplicity may be reduced if some final-state particles fail these acceptance cuts and/or if there are neutrinos in the final state.

The upper right panel of figure 4 shows the distribution in the sphericity, S_T, for sphaleron-induced final states with 10 and 14 final-state particles as red and blue histograms, respectively. Both distributions are relatively broad, being peaked at $S_T \sim 0.4$ and 0.6, respectively. The lower left panel of figure 4 displays histograms of the number of charged leptons, $N_{\mathrm{lep}} = N_e + N_\mu$, satisfying the nominal acceptance cuts. As expected, $N_{\mathrm{lep}} \leq 3$, with smaller numbers of charged leptons in events with final state neutrinos and/or charged leptons outside the nominal acceptance range. Finally, the lower right panel of figure 4 shows histograms of the numbers of top quarks in the sphaleron-induced final states. The most common outcome is to observe just one top quark, followed by final states with two top quarks. There are relatively few final states with no top quarks, and
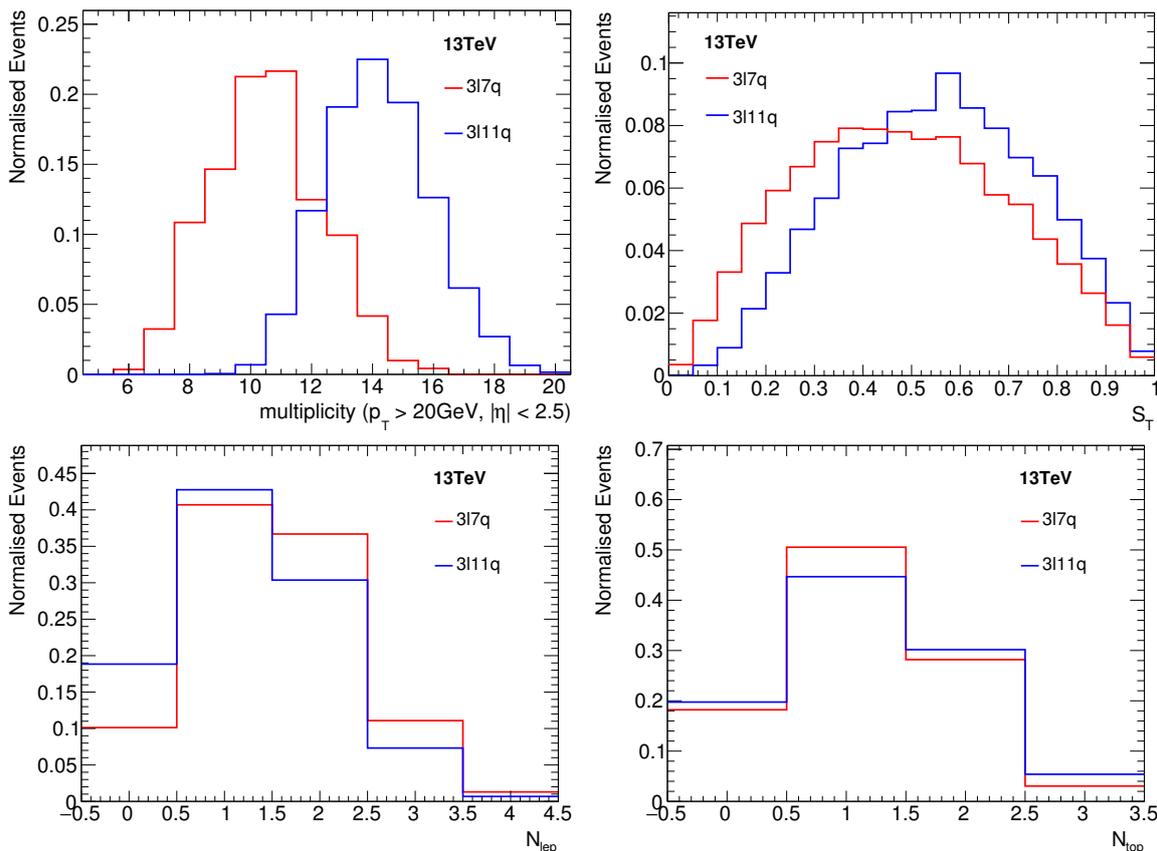
Figure 4. Left panel: normalized invariant-mass distributions for the observable final state particles in sphaleron-induced transitions in LHC collisions at 13 and 14 TeV (blue and red histograms, respectively). Right panel: corresponding invariant-mass distributions for future colliders at 33 and 100 TeV (green and pink histograms, respectively). These distributions are also calculated for our nominal choices $E_{\rm Sph} = 9$ TeV, $c = 2$ and $p = 1$.

even fewer with three top quarks. The difference between the cases with one and two top quarks is due to the phase-space suppression of final states with more top quarks than bottom quarks, as is that between the cases with zero and three top quarks.

Additional properties of 10-particle sphaleron final states are shown in figure 5, where we compare distributions at different LHC energies, 13 and 14 TeV, in the left panels (blue and red histograms, respectively), and possible future collider energies, 33 and 100 TeV, in the right panels (green and pink histograms, respectively). The upper panels display the distributions in $H_T \equiv \sum p_T^{\rm jet}$ and the lower panels the distributions in $E_T^{\rm miss}$, where the former is used in the ATLAS microscopic black hole search [22]. The H_T distributions at the two LHC energies are very similar, both being peaked at ~ 6 TeV. The distributions at the two future collider energies peak at somewhat higher energies ~ 7 TeV, but with longer tails at higher values of H_T, particularly at 100 TeV. The $E_T^{\rm miss}$ distributions at the two LHC energies are also very similar, both being peaked at ~ 0.5 TeV. The distributions at 33 and 100 TeV are also peaked at ~ 0.7 TeV, but with longer tails to higher values, particularly at 100 TeV.
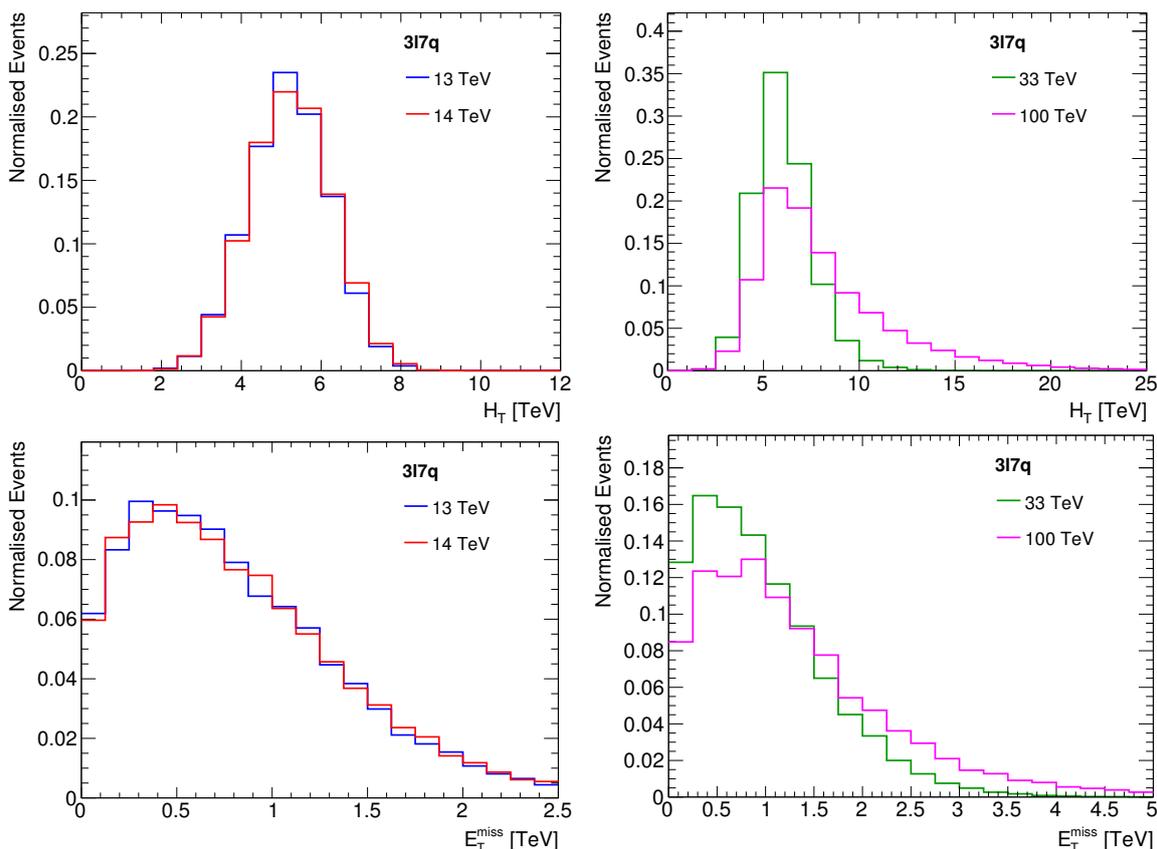
Figure 5. Upper panels: normalized distributions in $H_T \equiv \sum p_T^{\text{jet}}$ for the observable final state particles in sphaleron-induced transitions in LHC collisions at 13 and 14 TeV in the left panel and at 33 and 100 TeV in the right panel. Lower panels: normalized distributions in E_T^{miss} for the two LHC energies in the left panel and the two future collider energies in the right panel. Again, these distributions are calculated for our nominal choices $E_{\text{Sph}} = 9$ TeV, $c = 2$ and $p = 1$.

5 Analysis of ATLAS 2015 data

The ATLAS Collaboration has recently published the (null) results of a search for microscopic black holes using $\sim 3\,\text{fb}^{-1}$ of data at 13 TeV recorded in 2015 [22]. This analysis was based on measurements of the numbers of events in search regions (SRn_{jet}) defined by cuts in the number of jets with $p_T > 50\,\text{GeV}$ and $|\eta| < 2.8$: $n_{\text{jet}} \geq 3$ to 8, accompanied by cuts in $H_T \gtrsim 5\,\text{TeV}$. We now compare the ATLAS measurements with our parton-level simulations of the final states induced by sphaleron transitions. Although we neglect various effects such as parton showering, hadronization and detector resolution, we expect our limit is in a right ball-park, for the following reasons. As mentioned above, the event selection is based entirely on jets, for which the acceptance is almost 100% for signal jets with p_T much higher than the kinematical threshold of 50 GeV. The primary relevant effect of parton showering is the splitting of a quark momentum into two (or more) jets. However, H_T is not sensitive to this splitting, because it is defined inclusively as the sum of jet momenta ($H_T \equiv \sum p_T^{\text{jet}}$). Also this effect tends to increase the number of jets, which makes our limit only more conservative.
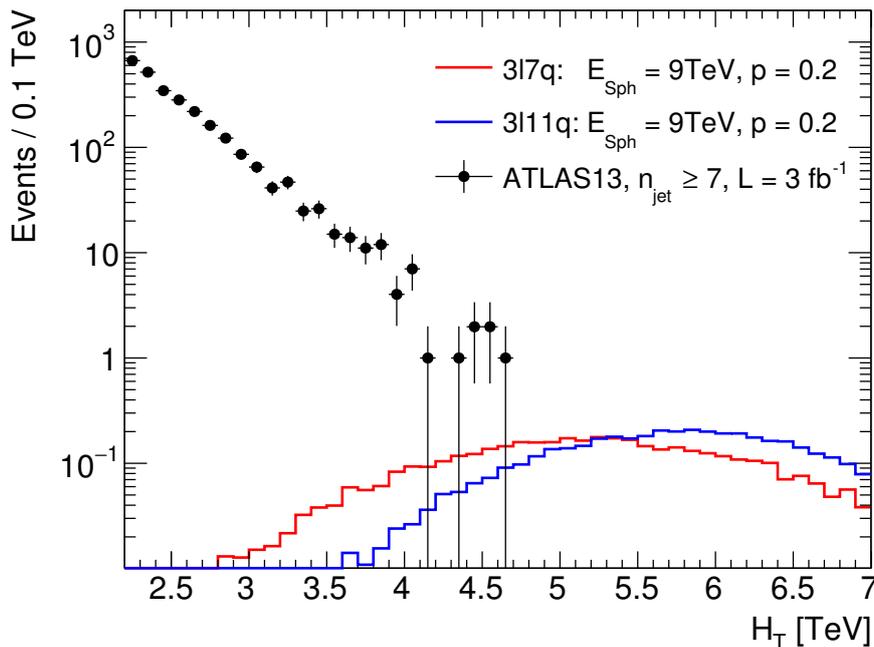
Figure 6. Comparison of the numbers of events with $n_{\text{jet}} \geq 3$ measured by ATLAS in $\sim 3/\text{fb}$ of data at 13 TeV in bins of H_T, compared with simulations for $E_{\text{Sph}} = 9\,\text{TeV}$ and $c = 2$ of $\Delta n = -1$ sphaleron transitions to final states with 3 antileptons and 7 antiquarks (red histogram) and $\Delta n = +1$ transitions to final states with 3 leptons and 11 quarks (blue histogram).

Figure 6 compares the ATLAS measurements for $n_{\text{jet}} \geq 7$ in bins of $H_T \leq 7\,\text{TeV}$ with sphaleron simulations for $E_{\text{Sph}} = 9\,\text{TeV}$ and $p = 0.2$ (the results are insensitive to c). We see that events due to sphaleron transitions are expected to have a broad distribution in H_T, with a large fraction having $H_T \gtrsim 5\,\text{TeV}$. We focus initially on the case of $\Delta n = -1$ transitions, which yield final states with 3 antilepton + 7 antiquarks (4.1), corresponding to the red histogram in figure 6. The corresponding values of the acceptances for these final states in the different ATLAS search regions SR3, ..., SR8 as functions of the sphaleron barrier height $E_{\text{Sph}} \in [8, 10]\,\text{TeV}$ are shown in the left panel of figure 7. We note that characteristic values of the acceptances for the nominal $E_{\text{Sph}} = 9\,\text{TeV}$ are $\gtrsim 0.4$ for SR6, SR7 and SR8.

We may therefore recast the ATLAS search as a relatively efficient search for $\Delta n = -1$ sphaleron-induced transitions. For each value of E_{Sph}, we select the SRn that is expected to yield the best limit, finding that SR8 is expected to be the most sensitive for $E_{\text{Sph}} \lesssim 9.3\,\text{TeV}$ whereas SR7 is the most sensitive for $E_{\text{Sph}} \gtrsim 9.3\,\text{TeV}$. The exclusion limit resulting from this recasting of the ATLAS black hole search is shown in the right panel of figure 7. We display the 95% CL constraint in the (E_{Sph}, p) plane, which is quite insensitive to $c \in [1, 4]$. We note that this preliminary result already excludes $p = 1$ for the nominal value of $E_{\text{Sph}} = 9\,\text{TeV}$.

Thus far, we have discussed $\Delta n = -1$ sphaleron transitions in which two quarks collide to yield 3 antileptons and 7 antiquarks, and now we consider the next simplest possibility of a $\Delta n = +1$ sphaleron transition in which two quarks collide to yield 3 leptons and 11
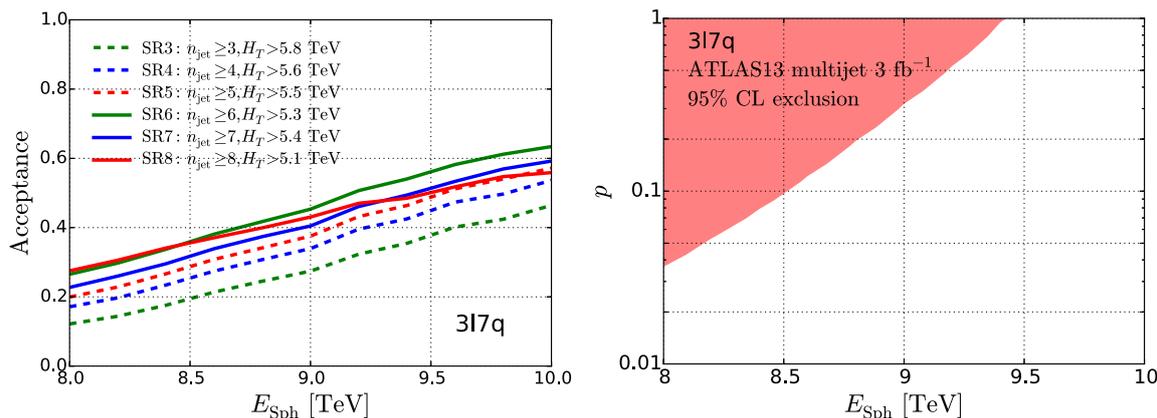
Figure 7. Right panel: acceptances for sphaleron-induced $\Delta n = -1$ transitions in ATLAS event selections with different cuts in (n_{jet}, H_T), as functions of E_{Sph}. Left panel: the exclusion in the (E_{Sph}, p) plane of $\Delta n = -1$ transitions obtained by recasting the ATLAS 2015 search for microscopic black holes using $\sim 3/\mathrm{fb}$ of data at $13\,\mathrm{TeV}$. The variation in the exclusion for $1 \leq c \leq 4$ is negligible.
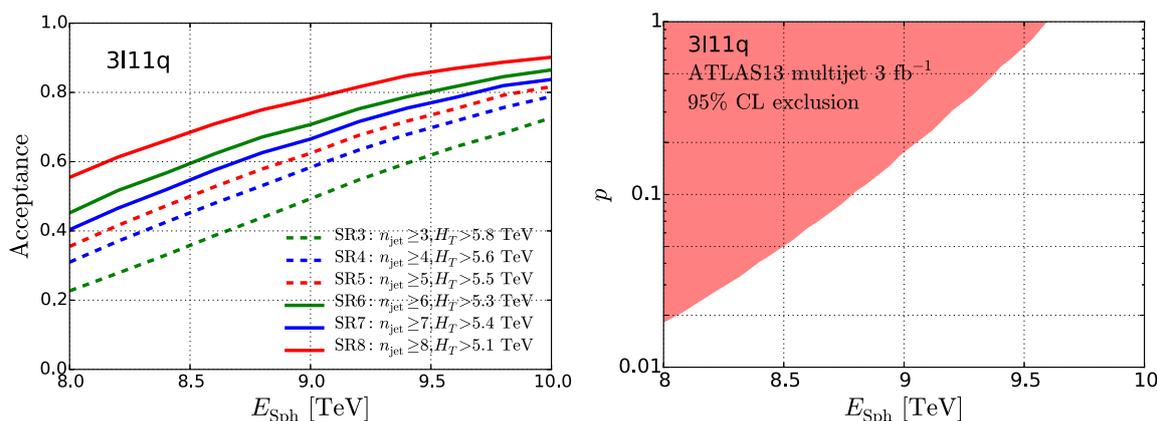
Figure 8. Left panel: acceptances as in right panel of figure 6, but for $\Delta n = +1$ sphaleron-induced transitions to 14-particle final states. Right panel: the exclusion in the (E_{Sph}, p) plane, as in figure 7 but for sphaleron-induced transitions to 14-particle final states.

quarks. The left panel of figure 6 shows the simulated H_T distribution for this possibility as a blue histogram, which is shifted to larger values than for the $\Delta n = -1$ sphaleron transitions. Correspondingly, the acceptances in the ATLAS search regions are higher for $\Delta n = +1$ transitions, as seen in the left panel of figure 8, reaching ~ 0.8 for SR8 for the nominal $E_{\mathrm{Sph}} = 9\,\mathrm{TeV}$. Consequently, the 95% CL exclusion in the (E_{Sph}, p) plane for $\Delta n = +1$ transitions is correspondingly stronger than for $\Delta n = -1$ transitions, as seen in the right panel of figure 8, excluding $p \simeq 0.2$ for the nominal $E_{\mathrm{Sph}} = 9\,\mathrm{TeV}$.[7]

---

[7]Similarly, there would be even stronger exclusions for $|\Delta n| > 1$ transitions.

6 Future prospects

Run 2 of the LHC is expected to yield $\sim 100\,\mathrm{fb}^{-1}$ of data at $13\,\mathrm{TeV}$, which should enable the sensitivity to p to be improved to ~ 0.01 for $E_{\mathrm{Sph}} = 9\,\mathrm{TeV}$, which could be improved with an optimized, targeted analysis of the final states in sphaleron-induced transitions.

For example, as was pointed out in [14], $\Delta n = -1$ sphaleron-induced processes would yield final states with multiple positively-charged leptons: e^+, μ^+ and/or τ^+. In particular, $1/8$ of the final states would contain the distinctive combination of all three positively-charged leptons: $e^+ + \mu^+ + \tau^+$. Also, every $\Delta n = -1$ sphaleron-induced event would contain 0, 1, 2 or 3 top antiquarks accompanied by 3, 2, 1 or 0 bottom antiquarks. Therefore, every sphaleron-induced final state should contain multiple bottom antiquarks, produced either directly or in antitop decays. Assuming the nominal value $E_{\mathrm{Sph}} = 9\,\mathrm{TeV}$, we have calculated the phase space factors for final states in $\Delta n = -1$ processes containing 1, 2 or 3 top antiquarks, which are reduced by 0.90, 0.75 and 0.62 relative to topless final states. Including combinatorial factors of 3 for the 1- and 2-top final states and the constraint of charge conservation and detector acceptance we found the ratios of 0-, 1-, 2- and 3-top final states to be $1 : 2.83 : 1.56 : 0.17$, as can be seen from the bottom right panel of figure 4. The final states containing top antiquarks may therefore provide distinctive signatures. Using such antilepton, bottom and top antiquark signatures might improve the Run-2 sensitivity significantly, particularly if both ATLAS and CMS searches could be combined.

The sensitivity could be further improved by a factor ~ 6 if the LHC could make collisions at $14\,\mathrm{TeV}$, and by another factor of 30 with $3000\,\mathrm{fb}^{-1}$ of luminosity, pushing the sensitivity to $p < 10^{-4}$ for $E_{\mathrm{Sph}} = 9\,\mathrm{TeV}$. The sensitivity could be further improved to $p \sim 10^{-11}$ for two experiments each with $20{,}000\,\mathrm{fb}^{-1}$ of luminosity at $100\,\mathrm{TeV}$ in the centre of mass. The fact that future searches at the LHC and a possible future collider have such interesting prospective sensitivities to sphaleron-induced transitions reinforces the importance of assessing the reliability of the TW estimate of the sphaleron transition rate. Both the exponential factor $S(E)$ and the pre-exponential factor p need close scrutiny. Our exploratory study shows that this is not just an academic study, but could have exciting implications for future pp collider experiments.

References

[1] A.A. Belavin, A.M. Polyakov, A.S. Schwartz and Yu.S. Tyupkin, *Pseudoparticle Solutions of the Yang-Mills Equations*, *Phys. Lett.* **B 59** (1975) 85 [INSPIRE].

[2] N.S. Manton, *Topology in the Weinberg-Salam Theory*, *Phys. Rev.* **D 28** (1983) 2019 [INSPIRE].

[3] F.R. Klinkhamer and N.S. Manton, *A Saddle Point Solution in the Weinberg-Salam Theory*, *Phys. Rev.* **D 30** (1984) 2212 [INSPIRE].

[4] A.H. Mueller, *On higher order semiclassical corrections to high-energy cross-sections in the one instanton sector*, *Nucl. Phys.* **B 364** (1991) 109 [INSPIRE].

[5] O. Espinosa, *High-Energy Behavior of Baryon and Lepton Number Violating Scattering Amplitudes and Breakdown of Unitarity in the Standard Model*, *Nucl. Phys.* **B 343** (1990) 310 [INSPIRE].

[6] A. Ringwald, *High-Energy Breakdown of Perturbation Theory in the Electroweak Instanton Sector*, *Nucl. Phys.* **B 330** (1990) 1 [INSPIRE].

[7] V.I. Zakharov, *Classical corrections to instanton induced interactions*, *Nucl. Phys.* **B 371** (1992) 637 [INSPIRE].

[8] S.Yu. Khlebnikov, V.A. Rubakov and P.G. Tinyakov, *Instanton induced cross-sections below the sphaleron*, *Nucl. Phys.* **B 350** (1991) 441 [INSPIRE].

[9] M. Porrati, *Dispersion Relations and Finite Size Effects in High-energy Electroweak Interactions*, *Nucl. Phys.* **B 347** (1990) 371 [INSPIRE].

[10] V.V. Khoze and A. Ringwald, *Total cross-section for anomalous fermion number violation via dispersion relation*, *Nucl. Phys.* **B 355** (1991) 351 [INSPIRE].

[11] V.A. Rubakov and M.E. Shaposhnikov, *Electroweak baryon number nonconservation in the early universe and in high-energy collisions*, *Usp. Fiz. Nauk* **166** (1996) 493 [hep-ph/9603208] [INSPIRE].

[12] A. Ringwald, *Electroweak instantons/sphalerons at VLHC?*, *Phys. Lett.* **B 555** (2003) 227 [hep-ph/0212099] [INSPIRE].

[13] A. Ringwald, *An Upper bound on the total cross-section for electroweak baryon number violation*, *JHEP* **10** (2003) 008 [hep-ph/0307034] [INSPIRE].

[14] S.H.H. Tye and S.S.C. Wong, *Bloch Wave Function for the Periodic Sphaleron Potential and Unsuppressed Baryon and Lepton Number Violating Processes*, *Phys. Rev.* **D 92** (2015) 045005 [arXiv:1505.03690] [INSPIRE].

[15] V.A. Kuzmin, V.A. Rubakov and M.E. Shaposhnikov, *On the Anomalous Electroweak Baryon Number Nonconservation in the Early Universe*, *Phys. Lett.* **B 155** (1985) 36 [INSPIRE].

[16] M. Fukugita and T. Yanagida, *Baryogenesis Without Grand Unification*, *Phys. Lett.* **B 174** (1986) 45 [INSPIRE].

[17] A.G. Cohen, D.B. Kaplan and A.E. Nelson, *Progress in electroweak baryogenesis*, *Ann. Rev. Nucl. Part. Sci.* **43** (1993) 27 [hep-ph/9302210] [INSPIRE].

[18] M. Trodden, *Electroweak baryogenesis*, *Rev. Mod. Phys.* **71** (1999) 1463 [hep-ph/9803479] [INSPIRE].

[19] D.E. Morrissey and M.J. Ramsey-Musolf, *Electroweak baryogenesis*, *New J. Phys.* **14** (2012) 125003 [`arXiv:1206.2942`] [ɪɴSPIRE].

[20] M.E. Shaposhnikov, *Baryon Asymmetry of the Universe in Standard Electroweak Theory*, *Nucl. Phys.* **B 287** (1987) 757 [ɪɴSPIRE].

[21] A. Ringwald and H. Tu, *Collider versus cosmic ray sensitivity to black hole production*, *Phys. Lett.* **B 525** (2002) 135 [`hep-ph/0111042`] [ɪɴSPIRE].

[22] ATLAS collaboration, *Search for strong gravity in multijet final states produced in pp collisions at $\sqrt{s} = 13$ TeV using the ATLAS detector at the LHC*, *JHEP* **03** (2016) 026 [`arXiv:1512.02586`] [ɪɴSPIRE].

[23] T. Akiba, H. Kikuchi and T. Yanagida, *Static Minimum Energy Path From a Vacuum to a Sphaleron in the Weinberg-Salam Model*, *Phys. Rev.* **D 38** (1988) 1937 [ɪɴSPIRE].

[24] P.B. Arnold and L.D. McLerran, *The Sphaleron Strikes Back*, *Phys. Rev.* **D 37** (1988) 1020 [ɪɴSPIRE].

[25] L.D. McLerran, A.I. Vainshtein and M.B. Voloshin, *Electroweak Interactions Become Strong at Energy Above Approximately 10-TeV*, *Phys. Rev.* **D 42** (1990) 171 [ɪɴSPIRE].

[26] M.J. Gibbs, A. Ringwald, B.R. Webber and J.T. Zadrozny, *Monte Carlo simulation of baryon and lepton number violating processes at high-energies*, *Z. Phys.* **C 66** (1995) 285 [`hep-ph/9406266`] [ɪɴSPIRE].

[27] M.J. Gibbs and B.R. Webber, *HERBVI: A program for simulation of baryon and lepton number violating processes*, *Comput. Phys. Commun.* **90** (1995) 369 [`hep-ph/9504232`] [ɪɴSPIRE].